Raman sideband cooling of rubidium atoms in optical lattice*

Chun-Hua Wei(魏春华)[1,2] and Shu-Hua Yan(颜树华)[1,2,†]

[1] College of Mechatronic Engineering and Automation, National University of Defense Technology, Changsha 410073, China
[2] Interdisciplinary Center for Quantum Information, National University of Defense Technology, Changsha 410073, China

(Received 23 February 2017; revised manuscript received 3 May 2017; published online 20 June 2017)

We develop a simple and practical scheme to apply sideband cooling to a cloud of rubidium atoms. A sample containing 4×10^{7} ^{87}Rb is trapped in a far red detuned optical lattice. Through optimizing the relevant parameters, i.e., laser detuning, magnetic field, polarization, and duration time, a temperature around 1.5 μK and phase space density close to 1/500 are achieved. Compared with polarization gradient cooling, the temperature decreases by around one order of magnitude. This technique could be used in high precision measurement such as atomic clocks and atom interferometer. It could also serve as a precooling means before evaporation cooling in a dipole trap, and may be a promising method of achieving quantum degeneracy with purely optical means.

Keywords: atom cooling, optical lattice, sideband cooling

PACS: 07.05.Fb, 37.10.De, 37.10.Jk **DOI:** 10.1088/1674-1056/26/8/080701

1. Introduction

Ever since the first sub-Doppler temperatures were observed in optical molasses,[1] experimenters have pushed laser cooling techniques towards lower temperatures at higher densities. For further cooling, it is usually necessary to scatter more cooling photons, which results in spontaneous emission. These photons are on resonance with other atoms in the sample, making it optically dense. Density dependent heating is a limiting factor in laser cooling. Once a cooling photon is scattered it possesses a random polarization and propagation direction, subject to conservation of linear and angular momentum. Thus, it cannot contribute to the laser cooling effect and instead heats each atom it re-scatters by one recoil energy $E_{\rm R}=\hbar^2k^2/2M$. In a dilute gas the photon is unlikely to scatter off very many atoms as it leaves the gas, so the heating effect is small. However, as the density of the gas increases, the number of scattering events before the photon leaves the sample is also small. The result is a net heating, rather than cooling, by that photon.[2] The second effect which must be considered is the effect of light-assisted inelastic collisions. When a large scattering rate generates a significant population of atoms in the excited state in a time of the order of a typical interaction event, the result is a strong susceptibility to strong dipole–dipole interaction in a light field.[3] For a blue-detuned laser this causes a repulsive potential and heating, while for a red-detuned laser it can result in excited molecular bound states.[4] Both cases result in significant heating of the atoms involved and loss of atoms from the trap.[3,5–7]

These limitations prompted the development of so-called "dark-state" cooling schemes, such as free space Raman cooling (FSRC), velocity selective stimulated Raman transitions,[8–10] blue-detuned Sisyphus cooling or "Grey Molasses",[11,12] dark spot magneto-optical trap (MOT),[13,14] and velocity selective coherent population trapping (VSCPT).[15] However, these techniques do not use true dark states. FSRC and VSCPT are velocity selective cooling, they make use of the Doppler shift to cool atoms to specific momentum states near zero momentum, which are then dark to the cooling photons. Grey optical molasses uses polarization gradients and optical pumping to dark m_F states to cool. A reduction in heating is achieved since the spontaneous absorption rate is lower for a blue-detuned laser. The last one is a "dark spot MOT", which physically places a hole in the middle of the repumping light of an MOT. Atoms fall into a hyperfine level which is dark to the cooling light, making them immune to density-dependent heating. This allows higher densities to be achieved, however does not necessarily lead to colder atoms, as the atoms in the middle of the trap are not actively cooled beyond thermalisation with the surrounding cloud.

In this paper, we describe our experiments with a laser cooling technique known as Raman sideband cooling,[16–18] which is extremely insensitive to the traditional limitations of laser cooling to low temperatures at high densities. Raman sideband cooling has been successfully applied to cooling ions.[19,20] It also has been proven to work for atoms like Cs,[21] K,[22,23] and Li,[24] etc. This paper is dedicated to elucidating the mechanisms behind sideband cooling to understand how it works. In particular, we explain how it is possible to prepare a dark state with an extremely narrow linewidth,

*Project supported by the National Natural Science Foundation of China (Grant No. 51275523), the Specialized Research Fund for the Doctoral Program of Higher Education of China (Grant No. 20134307110009), the Graduate Innovative Research Fund of Hunan Province, China (Grant No. CX20158015), and the Excellent Graduate Innovative Fund of National University of Defense Technology (NUDT) (Grant No. B150305).

†Corresponding author. E-mail: yanshuhua996@163.com

© 2017 Chinese Physical Society and IOP Publishing Ltd

which is the key to achieving lower temperatures with laser cooling than the present experiments have allowed. Also, we develop a recipe for how to apply sideband cooling to a cloud of rubidium atoms. This technique could be used as a precooling means for the evaporation in a dipole trap, where much higher initial phase-space densities and atomic collision rates should allow the Bose–Einstein condensates to produce in a time shorter than in conventional experiments.

2. Theory

To develop a Raman sideband cooling scheme for rubidium we must choose and use a particular set of states. This choice determines the laser frequencies needed, takes into consideration the optical pumping and magnetic field. The energy level diagram for ^{87}Rb is shown in Fig. 1. The natural choice for the ground hyperfine state is $|F=1\rangle$, since this reduces the number of m_F states we need to consider in our Raman transitions.

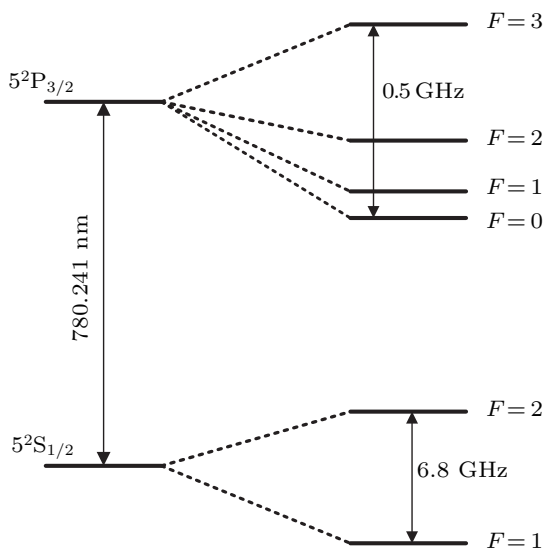


Fig. 1. Hyperfine splitting for the ^{87}Rb D_2 transition.

The dark state must be the high-field seeking m_F state, here the $|F=1,m_F=1\rangle$ state. We have freedom of choice over the excited state for optical pumping, the only requirement is that $|F=1,m_F=1\rangle$ can be made dark. This is most easily satisfied by pumping to the $|F'=0\rangle$ state of the excited hyperfine manifold. Then the dark state will be dark to both σ^+ and π light, allowing us to freely optically pump the $|F=1,m_F=-1,0\rangle \rightarrow |F'=0,m_F=0\rangle$ transitions without worrying about accidentally exciting atoms out of the dark state. This is, in fact, a specific case of a more general rule of thumb in sideband cooling: pumping on the $|F\rangle \rightarrow |F'=F-1\rangle$ transition, which is likely to produce more efficient cooling. In rubidium this is especially convenient as we can restrict ourselves to 3 different m_F states, which makes the cooling more robust. An adjusted sideband cooling scheme for rubidium is presented in Fig. 2. It is useful to notice that the narrow linewidth of the final spontaneous decay arises because of the transition to the dark ground vibrational state. The atom should receive a momentum kick from the emitted photon, however this is less than what is required to change the vibrational level.

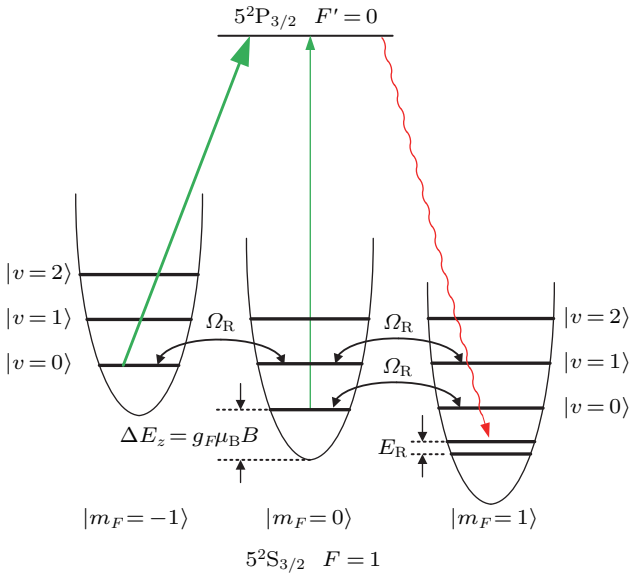


Fig. 2. (color online) A simple approach to degenerate Raman sideband cooling in ^{87}Rb, using the $5^2S_{1/2}$, $F=1$ ground state and $5^2P_{3/2}$, $F'=0$ excited state. The black curved arrows show the different degenerate Raman transitions between the $|m_F,v\rangle$ states, while the green arrows show the optical pumping to the excited states and the red arrow shows the spontaneous emission returning an atom to $|m_F=1\rangle$. The different m_F states necessitate the use of both $\sigma+$ and π light for optical pumping, or else atoms become stuck in $|m_F=0,v=1\rangle$ and will not be cooled further. The final spontaneous decay should be forbidden by conservation of momentum, since the recoil energy is not great enough to change the atom vibrational state. This gives the transition a narrow linewidth.

The Raman sideband cooling sequence proceeds as follows. First, a sample of ^{87}Rb atoms is cooled and prepared in the lower hyperfine ground state by using a standard MOT. The lattice is switched on, each atom is adiabatically loaded into a lattice site and occupies a set of vibrational states according to its initial momentum.

In the absence of a magnetic field the different m_F states are degenerate, however the introduction of a small magnetic field gives rise to a Zeeman splitting between the m_F states. This splitting can be tuned by using the magnetic field, so that the vibrational and magnetic splittings are the same, i.e., $\Delta E_{mF} = \Delta v = 1/2\hbar\omega_{\text{lattice}}$. The magnetic field (and quantisation axis) is chosen so that the $m_F = F$ magnetic sublevel is shifted down with respect to the $m_F = F-1$ sub level. The $|v=x,m_F=F\rangle$ and $|v=x-1,m_F=F-1\rangle$ states are then pairwise degenerate in total energy, except for the $|v=0,m_F=F\rangle$, which is lower in energy than all other states. This is shown in Fig. 2.

Once these levels are degenerate, 2-photon degenerate Raman transitions allow coupling between them. The photons driving this coupling can come from an external light

field, however for a lattice to be tuned close to resonance ($\sim$ 20 GHz) this 2-photon coupling is intrinsic to the lattice, with no external field required. The 2-photons in this process provide the linear and angular momentum necessary for an atom to change v and m_F states. The process is symmetric, atoms are pumped equally between the $|v = x, m_F = F\rangle$ and the $|v = x-1, m_F = F-1\rangle$ states so the steady state populations are the same.

This symmetry is broken by introducing state-dependent optical pumping. Optical pumping is arguably the most important part in the sideband cooling, as it is the key to cooling. The cooling effect in the ground state $F = 1$ hyperfine level is dependent on g_F, it determines the polarization of the optical pumping light needed (here σ^+). This is reversed in the other ground state hyperfine level ($F = 2$), where g_F has an opposite sign so that the atoms in that state will be heated instead of cooled. This provides another reason for choosing $F' = 0$ as our excited state, as the decay path from $|F = 1\rangle \rightarrow |F' = 2\rangle$ is forbidden due to angular momentum conservation. In spite of this, some atoms still decay to this state. Once there, they are not simply dark to cooling, they are heated from the sideband cooling scheme due to the different value of g_F for this state. This is remedied by providing a small amount of depumping light to prevent a population accumulating in this state. Conveniently, for ^{87}Rb, this transition can be reached experimentally by using the same light used for the magneto-optical trap.

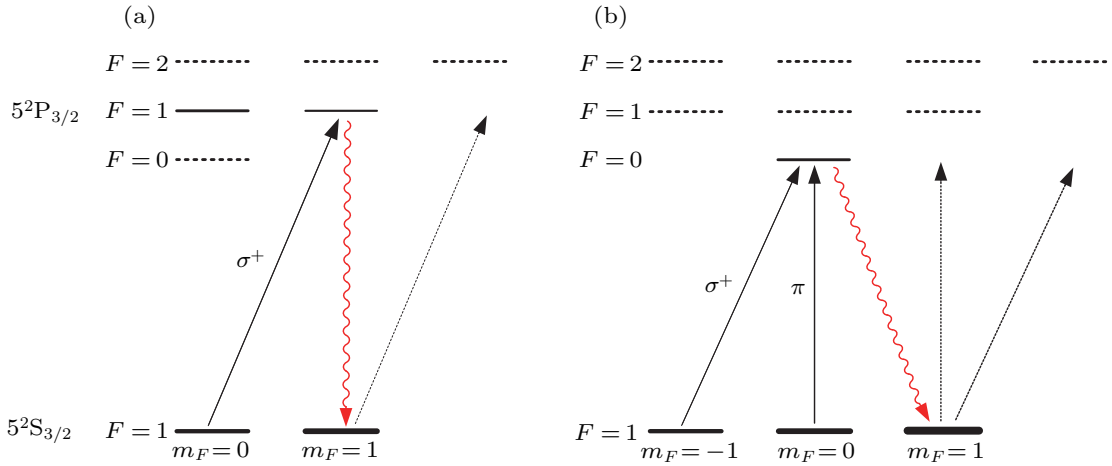


Fig. 3. (color online) Optical pumping between the $5^2S_{1/2}$ $F = 1$ ground state hyperfine level and the different excited state $5^2P_{3/2}$ hyperfine levels. Using $F' = 1$ for optical pumping requires only σ^+ light (a), while using $F' = 0$ requires both σ^+ and π polarized light (b). Using the $F' = 0$ state for optical pumping is superior, as it results in a darker $|m_F = 1\rangle$. This is because it is impossible to obtain pure σ^+ light at the atoms in our experiments, due to the phase shift in the light, induced by the glass cell and the subsequent π component is resonant for atoms in the m_F = 1 state. Pumping to $F' = 0$ does not suffer this problem as here $m_F = 1$ is dark to both σ^+ and π light. In addition to this, using $F' = 0$ reduces the need for depumping from the $F = 2$ ground state, as decays can only occur off-resonantly here.

Note that the recoil energy gained from the final electronic excitation is smaller than the vibrational spacings. It is typically unable to change the vibrational levels, which allows this whole process to lower the vibrational state of the atom and cool the sample, in addition to giving the excited state an artificially long lifetime. It is also important to note that the optical pumping step is crucial and without the spontaneous emission step the atom is able to just realize the transition between states without any actual cooling occurring.

3. Experiment and discussion

All the lasers in our system are external cavity diode lasers (ECDL), locked using saturated absorption spectroscopy (SAS). The trapping laser is amplified using a tapered amplifier (TA) to increase the power, and passes through a double pass acoustic-optic modulator (DP AOM), resulting in about 240 mW of trapping light to the glass cell. Immediately after the locking loop, a small amount of light is detuned using a DP AOM for use in imaging. This allows the imaging light to be tuned independently from the trapping light. The repump laser passes through an SAS and a single pass AOM, and the first order diffracted light is then fibre coupled to the glass cell with a total power of 12 mW. The zero order diffracted light passes through a double pass AOM and then fibre coupled to the glass cell used for optical pumping beam.

The laser used to generate the lattice is derived from an ECDL. It seeds a tapered amplifier (TA), which undergoes spatial filtering through a PM fibre before it goes to the cell. A home-built high fitness wave-meter[25] is added to easily and accurately detune the laser where we want. This allows the laser to be locked at any frequency by using a software PID and is experimentally simple to implement, as it requires only 10 μW of light coupled into the wave-meter fiber from the back of the SAS beamsplitter. In order to avoid spontaneous emission, the optical lattice is set to be 20-GHz detuning to the red of the resonance.

The intensity of the lattice is controlled directly by puls-

ing the current through the tapered amplifier through using a function generator (Agilent 33250A) and a Wavelength Electronics PLD5000 5A laser diode driver. This technique has been demonstrated before by Takase *et al.*,[26] and is useful for producing a high power output from a tapered amplifier when the limited seed light is available, or when the application only requires a large power for a short amount of time.

A polarized beam splitter is used to divide the total lattice power. Before the polarized beam goes into the cell, wave plates are placed to adjust the polarization of each lattice beam. We use three beams to build a two-dimensional (2D) lattice: a single beam retro-reflected back along its path, which passes vertically down through the cell. The third beam is held horizontally. All three beams are linearly polarized, with a $1/e^2$ waist of 5 mm.

Our experiment starts with an MOT capturing approximately 4×10^7 atoms in 200 ms. After atoms are trapped and cooled in the MOT, they are still too hot to be loaded into an optical lattice. It is necessary to cool them further by using polarization gradient cooling (PGC). In this process, the magnetic field is switched off, and the trapping light is detuned smoothly over 15 ms by using a linear ramp from 20 MHz to 100 MHz. The intensity of the light is not directly varied, however it does decrease due to the variation in the coupling efficiency between the AOM and the fibre. The intensity of the repump light is reduced during this ramp, to restrict the population in the $F=2$ ground state and increase the cooling effect of the PGC. After PGC there are 4×10^7 atoms at about 12 μK. Figure 7(a) shows the saturated absorption imaging of atomic diffusion at the time after PGC process. Figures 8(a) and 8(b) show the temperature fitting in the horizontal and vertical direction after PGC, respectively.

In order to realize the adiabatic loading and unloading, the lattice intensity must follow a specific functional form to avoid overheating the atoms.[27] The adiabatic loading and unloading of the lattice is demonstrated in Fig. 4. The atoms are loaded into the lattice with a 3-ms linear ramp which begins 3-ms before the end of PGC. For the figure, the atoms are held in the lattice (detuned 20 GHz to the red of $|F=2\rangle \rightarrow |F'=3\rangle$) for 10 ms after the MOT light has been extinguished, and then allowed to expand for 15 ms before they are imaged at resonance. The figure clearly shows that in this regime as the intensity of the lattice is increased it can hold more atoms.[28] Additionally, at this detuning the atom number remains constant for all powers.

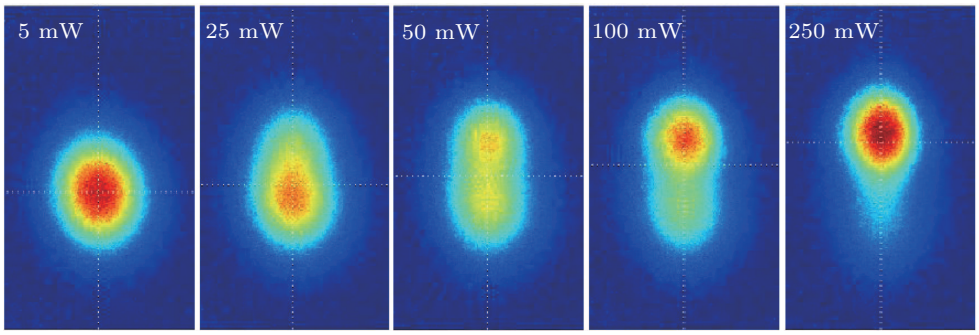


Fig. 4. (color online) Adiabatically loading process of the optical lattice with red detuning of 20 GHz. Trapped atoms are loaded adiabatically by using a 3-ms linear ramp beginning 3 ms before the end of the PGC. Atoms are held in the lattice for 10 ms, and then released adiabatically to free flight for 15 ms before imaging, so that the top and bottom atom clouds have drop times of 15 ms and 25 ms respectively.

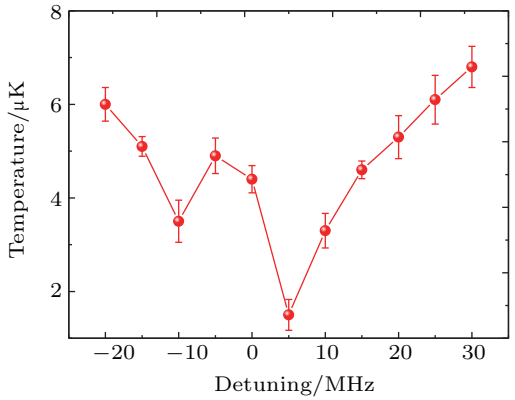


Fig. 5. (color online) Temperature of laser-cooled atoms as a function of pumping beam detuning.

The lattice loading is overlapped with the end of PGC, after that, the molasses laser beams are extinguished, leaving the atoms in the optical lattice only. The magnetic field and optical pumping beam turn on 3 ms later after the lattice beam has turned on.

For the best cooling, all the parameters should be optimized. Figure 5 gives the cloud temperature as a function of optical pumping beam detuning. Positive numbers represent blue detuning, negative numbers means red detuning, and the angle between the magnetic field and optical pumping beam is 10°. At 5-MHz blue detuning from the $|F=1\rangle \rightarrow |F'=0\rangle$, we obtain the best cooling result.

The magnetic field, used to produce Zeeman splitting between the m_F states, is generated from the compensation coils. The angle between the magnetic field and optical pumping beam is typically chosen to be in a range of 5°–20°, resulting

in I_π/I_σ ranging from 0.7% to 13%. Figure 6 shows the cloud temperature as a function of magnetic field. Note that the direction of the magnetic field is fixed, the angle between the magnetic field and optical pumping beam is adjusted through changing the direction of the pumping beam.

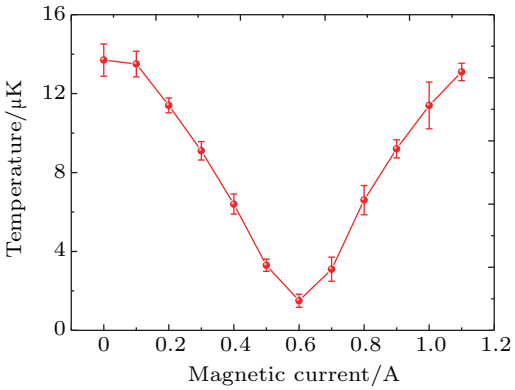


Fig. 6. (color online) Temperature of laser-cooled atoms as a function of magnetic field.

The duration of the cooling, with optical pumping and magnetic field being both on, is optimized to be 15 ms, after which the optical pumping is extinguished with an AOM in ~ 1 μs, and the magnetic field is brought to zero within ~ 100 μs. Then, the cloud is adiabatically released from the lattice. Figure 7(b) shows the saturated absorption images after Raman sideband cooling process. Comparing with Fig. 7(a), it is clearly shown that the cloud is colder as the diffusion is less. Figures 8(c) and 8(d) give the fit results of horizontal and vertical temperature after sideband cooling.

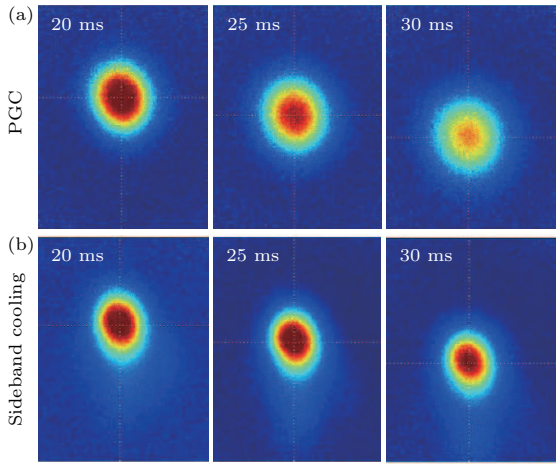


Fig. 7. (color online) Saturated absorption images of atomic diffusion with time after (a) free space PGC process, (b) Raman sideband cooling in a 2D optical lattice. Images are taken at resonance using absorption imaging. The drop times are given from switching off both the magnetic field and the trapping light.

Taking advantage of the sideband cooling in optical lattice, the temperature cools down to around 1.5 μK from 12 μK after PGC in less than 20 ms. The cloud density after PGC is 1.6×10^{11} atoms/cm^3, and after sideband cooling, the density is around 1.4×10^{11} atoms/cm^3, which means that the sideband cooling in optical lattice has a feeble effect on the density. Since the temperature decreases by around one order of magnitude and the density has only a small change, the phase space density will increase more than one order of magnitude.

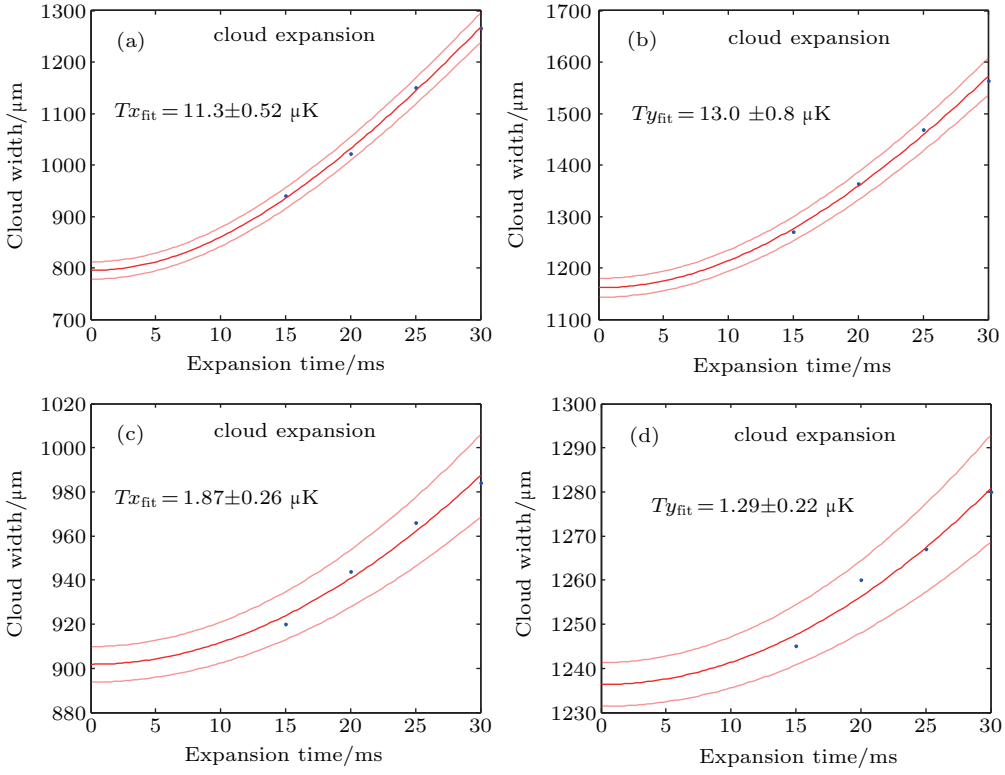


Fig. 8. (color online) Many runs are taken to obtain statistics for the width of the cloud after different drop times. [(a), (b)] Temperature fits of PGC, [(c), (d)] temperature fits of sideband cooling. These are used to fit a temperature curve (solid red line) as well as determine the 90% confidence intervals on this fit (dashed red lines).

4. Conclusions

In conclusion, we developed a simple and powerful atomic cooling method in far-detuned optical lattices that achieves much lower atomic temperature than optical molasses, and produces high phase-space density in the meantime. Sideband cooling is highlighted as a suitable replacement, allowing a larger atom number to be cooled to temperatures comparable to those obtained through RF evaporation in a magnetic trap. The ability to achieve low temperature and high phase space density within a short time opens the door for high precision measurement applications such as atomic clocks or atom interferometer, it could also be used as a precooling means before evaporation cooling to obtain BECs, and may be a promising method of achieving quantum degeneracy with purely optical means.

Acknowledgment

We would like to thank all colleagues from Atom Laser Group in Australia National University, especially Dr. Carlos Kuhn and Prof. Nick Robins, for enlightening discussion and technical support.

References

[1] Lett P D, Watts R N, Westbrook C I, Phillips W D, Gould P L and Metcalf H J 1988 *Phys. Rev. Lett.* **61** 169
[2] Cooper C J, Hillenbrand G, Rink J, Townsend C G, Zetie K and Foot C J 1994 *Europhys. Lett.* **28** 39
[3] Dashevskaya E I, Nikitin E E, Voronin A I and Zembekov A A 1970 *Can. J. Phys.* **48** 981.
[4] Kerman A J 2002 "Raman Sideband Cooling and Cold Atomic Collisions in Optical Lattices," Ph. D. Dissertation (Stanford University)
[5] Burnett K, Julienne P S and Suominen K A 1996 *Phys. Rev. Lett.* **77** 1416
[6] Julienne P 1996 *Journal of Research of the National Institute of Standards and Technology* **101** 487
[7] Weiner J, Bagnato V S, Zilio S and Julienne P S 1999 *Rev. Mod. Phys.* **71** 1
[8] Davidson N, Lee H J, Kasevich M and Chu S 1994 *Phys. Rev. Lett.* **72** 3158
[9] Kasevich M, Weiss D S, Riis E, Moler K, Kasapi S and Chu S 1991 *Phys. Rev. Lett.* **66** 2297
[10] Reichel J, Morice O, Tino G M and Salomon C 1994 *Europhys. Lett.* **28** 477
[11] Boiron D, Michaud A, Lemonde P, Castin Y, Salomon C, Weyers S, Szymaniec K, Cognet L and Clairon A 1996 *Phys. Rev. A* **53** R3734
[12] Boiron D, Trich C, Meacher D R, Verkerk P and Grynberg G 1995 *Phys. Rev. A* **52** R3425
[13] Ketterle W, Davis K B, Joffe M A, Martin A and Pritchard D E 1993 *Phys. Rev. Lett.* **70** 2253
[14] Townsend C G, Edwards N H, Zetie K P, Cooper C J, Rink J and Foot C J 1996 *Phys. Rev. A* **53** 1702
[15] Aspect A, Arimondo E, Kaiser R, Vansteenkiste N and Cohen-Tannoudji C 1988 *Phys. Rev. Lett.* **61** 826
[16] Monroe C, Meekhof D M, King B E, Jefferts S R, Itano W M, Wineland D J and Gould P 1995 *Phys. Rev. Lett.* **75** 4011
[17] Mnoret V, Geiger R, Stern G, Zahzam N, Battelier B, Bresson A, Landragin A and Bouyer P 2011 *Opt. Lett.* **36** 4128.
[18] Wolf S, Oliver S J and Weiss D S 2000 *Phys. Rev. Lett.* **85** 4249
[19] Poulsen G, Miroshnychenko Y and Drewsen M 2012 *Phys. Rev. A* **86** 051402
[20] Seck C M, Kokish M G, Dietrich M R and Odom B C 2016 *Phys. Rev. A* **93** 053415
[21] Han D J, Wolf S, Oliver S, McCormick C, DePue M T and Weiss D S 2000 *Phys. Rev. Lett.* **85** 724
[22] Grobner M, Weinmann P, Kirilov E and Nagerl H C 2017 *Phys. Rev. A* **95** 033412
[23] Cheuk L W, Nichols M A, Okan M, Gersdorf T, Ramasesh V V, Bakr W S, Lompe T and Zwierlein M W 2015 *Phys. Rev. Lett.* **114** 193001
[24] Parsons M F, Huber F, Mazurenko A, Chiu C S, Setiawan W, Wooley-Brown K, Blatt S and Greiner M 2015 *Phys. Rev. Lett.* **114** 213002
[25] White J D and Scholten R E 2012 *Rev. Sci. Instrum.* **83** 113104
[26] Takase K, Stockton J K and Kasevich M A 2007 *Opt. Lett.* **32** 2617
[27] Kastberg A, Phillips W D, Rolston S L, Spreeuw R J C and Jessen P S 1995 *Phys. Rev. Lett.* **74** 1542
[28] Wei C H, Yan S H, Yang J, Wang G C, Jia A A, Luo Y K and Hu Q Q 2017 *Acta Phys. Sin.* **66** 010701 (in Chinese)